SENSORLESS SPEED MEASUREMENT ASSOCIATED TO ELECTRONIC CONTROL BY THE LOAD FOR INDUCTION TURBOGENERATORS

Felix Alberto Farret, Jonas Rodrigues Gomes and Cesar Ramos Rodrigues
Universidade Federal de Santa Maria
Centro de Tecnologia
Programa de Pós-Graduação em Engenharia Elétrica
Faixa de Camobi, km 9 - Santa Maria, RS
Tel. (+55-55) 220.8456 FAX +55 55 220 8030 - ffarret@ct.ufsm.br

Abstract: **This paper discusses the application of a sensorless speed estimation algorithm based on the terminal voltage measurement of induction generators. This algorithm can be used as a reference to the control circuitry so replacing any rotor speed measurement, such as shaft encoders, by some few instructions in the microcontroller program. Such method is mostly suited for heuristic control methods as the Hill Climbing where the rotor speed is used to determine the safe operating area. These results seems to be acceptable inside the safe operating area since the terminal voltage magnitude keeps nearly proportional to the rotor speed.**

I. INTRODUCTION

The most attractive feature of powerplants using renewable sources of energy is their low cost. Therefore, the challenge is to make them to behave in the most appropriate way without adding unnecessary costs in any ways, either in its operation or when building it. It is known from the experience in designing powerplants that the control circuitry stands up for roughly 50% of the total plant cost. The other 50% are reserved for the generator and the turbine. Out of these costs, about 15% should be reserved for data acquisition. So, every alternative of good performance and cost reduction of the control circuitry should be seriously considered including here rotor speed measurement.

There are two main reasons for measuring and controlling the rotor speed. One is related to the mechanical overspeeding limits of the machine (either for generator or turbine). The other reason is when there is a need for tight control on the electrical frequency, since an extreme low rotor speed may lead to poor performance of the electrical parameters. Above all, it should be taken into account that every electrical machine has its optimum rotor speed for higher efficiency. There are many more or less precise alternatives of doing that.

One such alternative is a sensorless speed monitoring with purposes of control and measurement, particularly when the power plant uses "electronic control by the load". This control method is based on the difference between the total generated current and the current drawn by the main load to regulate its speed and output voltage, current or power. Furthermore, they totally replace the expensive conventional mechanical flux control of the primary source of energy and its associated voltage control[1,2]. It is not relevant if the micro-powerplant is used for power injection into the public network or as an isolated scheme. The scheme proposed in this paper is intended to be used in developing an algorithm to allow replacement of the shaft encoder by some few instructions in the microprocessor main control program. It is expected that the algorithm may be used for most of the small electrical machines and, in particular, for self-excited induction generators (SEIG) without mechanical speed or voltage control.

II. OPERATING PRINCIPLE

For establishing the operating principle of this sensorless measurement algorithm one should realize that the rotor speed is determined mostly by the generated active power. Bearing that in mind, a SEIG was connected to a diode power rectifier to feed a main load and a secondary load, both connected as shown in Figure 1. This figure shows the equivalent circuit of a micro-powerplant under the control viewpoint and of the values of current, voltage or power. Therefore, the induction generator terminals see an almost purely resistive load, that is, the active power to be controlled. To have generalized results, the main load was replaced by an ideal current source, as shown in Figure 1.

One way of relating the output voltage to the rotor speed is to previously map all possible speed conditions of the machine. To every change in the primary energy level for a given load current, there is a corresponding change in the rotor speed and, as a consequence, in the output voltage level.

The classical equations for DC-links can be adapted to relate load current, I_{dc}, and rotor speed, n_r. As the DC-side current is determined by the AC-side current through the AC source impedance, it is possible to evaluate the average voltage drop across the load terminals. From there, neglecting all harmonics and taking into account the relationship between V_{phase} and I_{dc}, the rectifier output voltage V_{dc} may be expressed as[5]:

$$V_{dc} = V_{do} - R_c I_{dc} \tag{1}$$

Where: R_c is the equivalent resistance of the rectifier, which includes the commutating resistance, the winding resistance, the diode resistance and the resistance of all connections.

$$V_{do} = \frac{3\sqrt{2}\sqrt{3}}{\pi} V_{fase}$$

$$I_2^2 R_2 \frac{1-s}{s} + I_2^2 (R_1 + R_2) + \frac{V_f^2}{R_m} + \frac{V_f^2}{R_{Lp}} = 0 \qquad (2)$$

$$\frac{V_f^2}{X_p} + \frac{V_f^2}{X_m} - \frac{V_f^2}{X_c} + \frac{V_f^2}{X_{Lp}} = 0 \qquad (3)$$

where:

$$s = 1 - \frac{n_r}{n_s}$$

$$X_m = \omega_s L_m .$$

First term of Equation 2 represents the converted mechanical energy, its signal being positive or negative (s > 1 or s < 0) if the mechanical power is coming out or going into the circuit.Diving Equation 3 by I_2^2 and simplifying it results:

$$\frac{R_2}{s} + R_1 + \frac{V_f^2}{I_2^2} \frac{1}{R_{mL}} = 0 \qquad (5)$$

where:

$$\frac{1}{R_{mL}} = \frac{1}{R_m} + \frac{1}{R_{Lp}}$$

From Equation 5 and Figure 4 it may be taken:

$$\frac{V_f^2}{F^2 I_2^2} = \left(\frac{R_2}{Fs} + \frac{R_1}{F}\right)^2 + (X_1 + X_2)^2 \qquad (6)$$

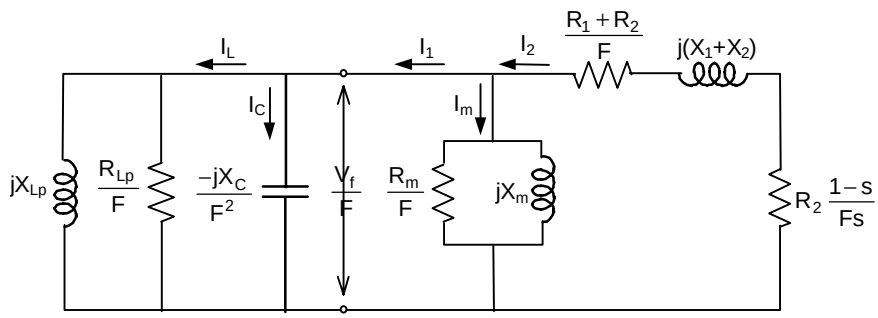

Figure 4 - Equivalent circuit including load and self-exciting capacitor

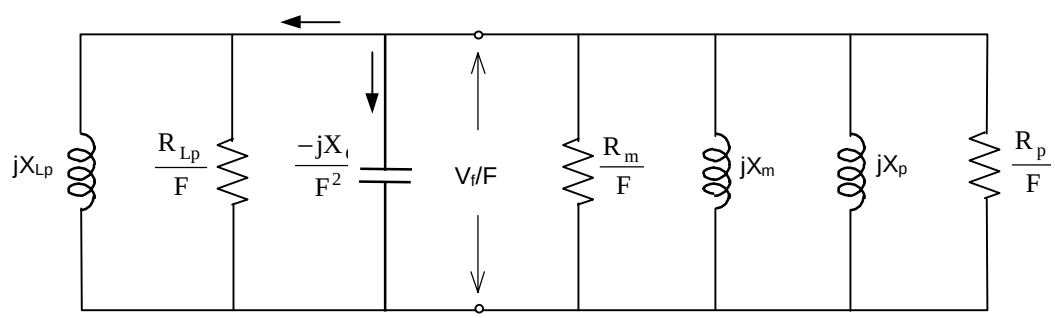

$$R_p = \frac{\left(\frac{R_1}{F} + \frac{R_2}{Fs}\right)^2 + (X_1 + X_2)^2}{R_1 + \frac{R_2}{s}} \qquad X_p = \frac{\left(\frac{R_1}{F} + \frac{R_2}{Fs}\right)^2 + (X_1 + X_2)^2}{X_1 + X_2}$$

Figure 5 - Simplified Doxey model for the self-excited induction generator

and so, Equation 5 becomes:

$$\frac{R_2}{s} + R_1 + \left[\left(\frac{R_2}{s} + R_1\right)^2 + F^2 (X_1 + X_2)^2\right] \frac{1}{R_{mL}} = 0$$

or

$$\left(\frac{R_2}{s} + R_1\right)^2 + \left(\frac{R_2}{s} + R_1\right) R_{mL} + F^2 (X_1 + X_2)^2 = 0 \qquad (7)$$

Assuming constant all the other machine parameters, Equation 7 becomes a second order equation which is useful to express the sliding figure for a given set of primary power and output load as:

$$s = \frac{2R_2}{-2R_1 - R_{mL} \pm \sqrt{R_{mL}^2 - 4F^2 (X_1 + X_2)^2}} \qquad (8)$$

This equation may be further simplified if it is considered that $R_{mL}^2 >> 4F^2 (X_1 + X_2)^2$ and that, in practice, R_{mL} must have a heavy, and not otherwise, influence on s. So, with a positive square root, we have:

$$s \cong -\frac{R_2}{R_1 + R_{mL}} \tag{9}$$

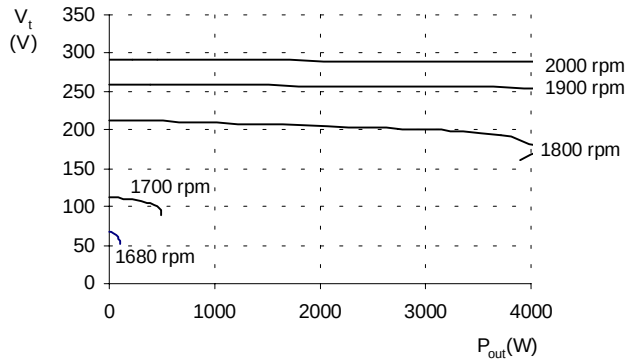

Figure 6 - Theoretical effects of the rotor speed on the output voltage and load

A numerical process may become necessary if Equation 8 is used rather than Equation 9, because the p.u. frequency, F, depends on ω_s that depends on s, which depends again on F.

The magnetizing reactance may be obtained from:

$$X_m = \frac{1}{F^2 \omega_s C - \frac{1}{X_p} - \frac{1}{X_{Lp}}} \tag{10}$$

IV. Experimental Results

This section discusses practical ways of implementing the control of rotation and of the output electrical variables (load) by simulating some typical situations. An PWM-IGBT circuit using pulse width modulation, W, was used to distribute the overall energy between primary and secondary loads. An induction motor of 220/380 V, 15/26 A, 1765 rpm, 7.5 hp was used for the practical and theoretical tests.

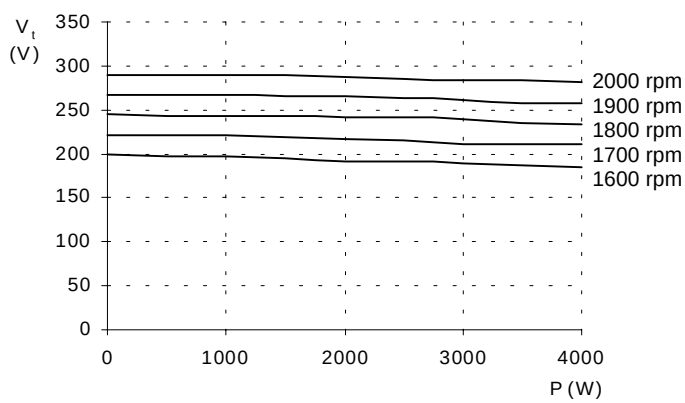

Figure 7 - Laboratory measurements of the rotor speed effects on the output voltage and load

Results obtained so far, from laboratory tests and from Excel (see Figures 7 and 8), for similar machine parameters, confirm the theoretical predictions and they give guidelines for the construction of a safe operating area. The limits of this safe area are related to: a) the maximum output voltage; b) the maximum mechanical rotor speed; c) the minimum excitation voltage and d) the minimum mechanical rotor speed under reasonable operating efficiency.

Figure 7, 8 and 9 show how proportional the output voltage changes are with respect to the active power under rotor speeds ranging from 1600 to 2000 rpm. The hatched area in Figure 8 suggests some limits for the safe rotor speed area imposed by the machine operating parameters related to the output power, rated voltage and rotor speed. Plot differences between theoretical and practical tests in Figure 7 and 8 are due to differences in the rated values of the commercial excitation capacitor which this correspond exactly to plate values (177 μF).

Practical results are plotted in Figure 7 and 9. It is noticeable that there is a strong relationship between the output voltage and the rotor speed as expected and that a safe operating area limits may be well established as already discussed above. For P_{out} = 1.0 pu it is almost linear such relationship, as shown in Figure 8.

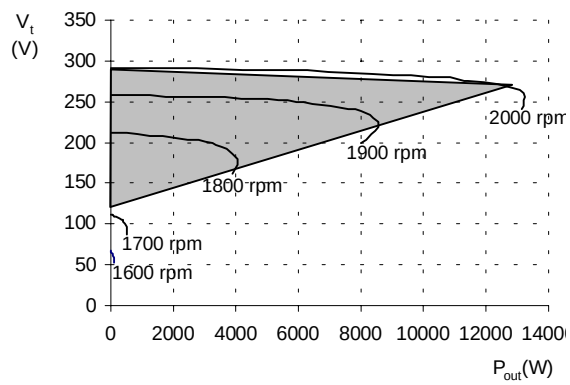

Figure 8 - Safe area for a sensorless rotor speed control

To have good performance of the electronic sensorless control, it is necessary to compare the levels of voltage, current or power and rotation to some reference level from which the control voltage is obtained for the electronic driving circuit. By using techniques of artificial intelligence in the control loop, it is possible to let the microcontroller to determine the safe area bonds. The principle based on the configuration shown in Figure 1 and theoretical results of Figure 9, illustrate how to vary the secondary resistor, R_2, from its nominal value to an almost open-circuit and so, having control on the rotor speed through load active power.

So, from Figures 7 through 9 it is possible to preliminarily conclude: I) though encouraging the preliminarily results, there is still some work to be done to improve the predictions of Equation 5 for the sensorless algorithm; II) there is not much distortion caused by core

between 80% to 110% of the nominal value (220V). Within these values, one obtains good flexibility to keep constant V_{dc} by a fine duty cycle adjustment. Furthermore, there will have a corresponding variation of the turbogenerator rotation because the DC voltage acts directly on the active power, as it will discussed in the practical results.

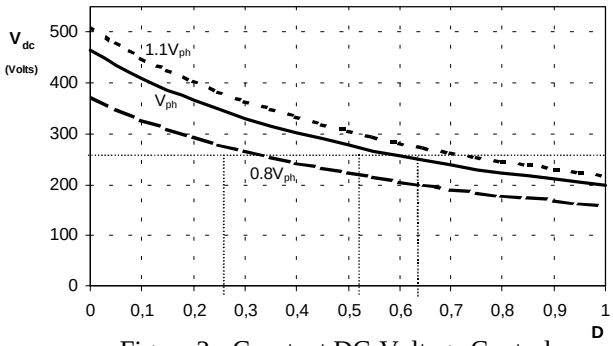

Figure 2 - Constant DC-Voltage Control

C. Simultaneous Voltage and Sensorless Speed Control by the Turbogenerator Load Power

An alternative way of controlling rotation together with the load voltage is by controlling the active power. Again, from Equation 1, the average load power is given by:

$$P = (V_{do} - R_c I_{dc})I_{dc} \tag{13}$$

where:

$$I_{dc} = \frac{V_{do}}{R_c + R_p} \tag{14}$$

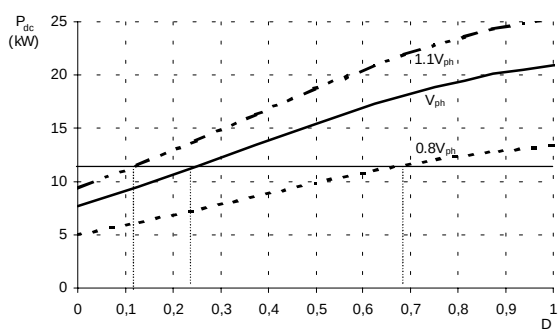

Figure 3 - The DC Power Control

Replacing equation 14 into 13 and rearranging everything, it comes:

$$P_{dc} = \frac{(R_1 D + R_2)R_1 R_2 V_{do}^{\ 2}}{[(R_1 D + R_2)R_c + R_1 R_2]^2} \tag{15}$$

Plots of Equation 15 presented in Figure 3 show how the load power can be kept constant (P_{dc} = 11,5 kW) at the same time that the active power absorbed by the generator is controlled.
For variations between D = 0.11 and D = 0.68, the control flexibility is sufficient for a wide variation of primary energy. Also, the smaller the R_c values the most noticeable are the DC power changes. These characteristics are very important when related to the "Hill Climbing Control" for maximum power generation[3].It should be noticed that the demanded power is smaller than the maximum primary energy available in the nature. One case where the maximum generated power is demanded, is the induction generation with an electronic control by the load. The design of such power plants and its operation allows a maximum power transfer to the load. The Point of Maximum Generated Power (PMGP) is determined by intersection between the characteristics of the primary energy source and of the load through a continuous increment (or decrement) of the load current[2]. This intersection point varies in time with the source and load conditions. For micro-powerplants, search of this operating point is justified by the fact that if all the energy is not used at the moment it is available in the nature (water level, water flow, wind speed, solar intensity, etc.), it will be wasted.

III. Approximate Analysis of the Induction Generator Performance

A simplified relationship between the output voltage and the rotor speed may be established from the classical model for either the self-excited or network-excited induction generators, as shown in Figure 4. This study is based on the model of Doxey which departures from the steady state induction machine analysis. As the exciting impedance is a lot larger than any other in the model is better to consider the simplified model presented in Figure 5 on which is already included the load and the self-exciting capacitor.[2]

Notice in Figure 5 that an inductive load affects negatively the effective value of the exciting capacitive reactance expressed as:

$$X_{Crms} = \frac{1}{j\omega_s [C - \frac{L}{R_L^2 + (\omega_s L)^2}]} \tag{1}$$

where:

ω_s is the stator speed
R_L, L are the load impedance parameters
C is the self-exciting capacitance

Influence of L on the exciting capacitor is definitely serious because it can put the capacitive reactance line over the linear portion of the no-load characteristic causing an output voltage collapse. The positive side of that is a very limited short-circuit current. On the other hand, a higher exciting capacitance may lead to an output current higher than the rated machine values.

Theoretical predictions of the machine performance may be conducted taking into account that the only active power is transferred from the primary source of energy. Reactive power balance is a null. Figure 4 and 5 may be used for calculation of the active and reactive powers yielding:

So, the open DC-link voltage, V_{do} , is closely related to the rotation of the primary machine, which is, by its turn, dependant on the available amount of primary energy with respect to the energy demand of the generator.

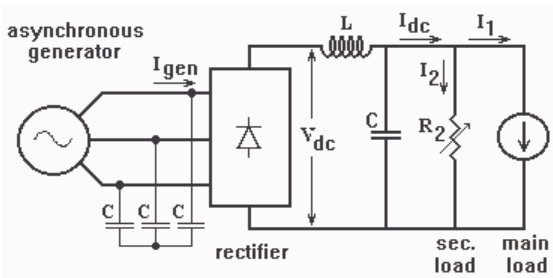

Figure 1 - Operating Principle of the Sensorless Measurement by the Load Current

Equation 1 expresses V_{dc} as a function of I_{dc} and of the internal converter voltage drops. Therefore, if the average output current of the rectifier is controlled, the generator load and, as a consequence, the turbogenerator speed will be controlled. The output voltage is directly related to its speed being irrespective to the type of main load current drain (either forced or naturally commutated converter or passive loads) as long there is a drain of current.

The variable resistance across the load terminals is responsible for the exceeding current control using a pulse width modulation (PWM). The point is to act on I_{dc} in order to control the turbogenerator speed and, consequently, the voltage V_{dc} and so, the main load voltage[1,3]. Three basic cases are discussed in the following sections.

A. Voltage and Speed Control by the Load Current[2,3]

From Figure 1 is also possible to understand the switching principle using a DC-DC converter with a PWM modulation to distribute the total generated current, I_{dc}, between the main current and the secondary current. Current I_2 is controlled by the effective value of resistor R_2, which controls I_2 to be diverted from the main load, to control I_{dc} and/or the main load current. All the same, to keep constant the main load current, I_1, during any primary source energy variation, I_2 should be compensated with identical variations but of opposite sign. If both, I_{dc} and I_1, should vary, the DC-DC converter must be able to compensate them according to its needs. The result could be seen as if there was an apparent independence between variations of the average DC-link current and the main load current whose difference is drained out by I_2:

$$I_{dc} = I_1 + I_2 \tag{6}$$

where: I_{dc} is the average DC link current;
I_1 is the average main load current; and
I_2 represents the average current through the secondary load.

The main load current variation must be compensated by an effective variation of the current through the variable resistor. In the laboratory model PWM modulation was used. For these purposes, the duty cycle is defined as:

$$D = \frac{W}{T} \tag{7}$$

where W is the pulse width of the current through the DC-DC converter, T_{sw} is the switching period. The converter secondary current is given by:

$$I_2 = \frac{D \times V_{cc}}{R} \tag{8}$$

where R_2 is the actual value of the secondary load. The effective value is given by:

$$R_2 = \frac{R}{D} \tag{9}$$

Combining equations 7 to 9, the control variable W may be obtained. It modulates the secondary resistor:

$$W = \frac{R_2}{f_{sw} V_{dc}} (I_{dc} - I_1) \tag{10}$$

From equations 1-5, relationship between I_{dc} and f_{sw} is given then as:

$$I_{dc} = \frac{V_{do}}{R_c + \dfrac{R_1 R_2}{R_1 W f_{sw} + R_2}} \tag{11}$$

B. Turbogenerator Voltage and Speed Control by the Load Voltage

The output voltage, V_{dc}, is a result of the interaction between I_{dc} and I_1 and from Figure 1 it can be seen that:

$$V_{dc} = \frac{R_p}{R_p + R_c} V_{do} \tag{11}$$

where R_p is the parallel combination between the equivalent main load resistor R_1 and the secondary resistor, R_2 , whose effective value is R_{2ef}.

The switching frequency is limited by the size of T_{sw} = W. Therefore, from equation 10 and 11 and Figure 1 one obtains:

$$V_{dc} \frac{1}{1 + \dfrac{R_c}{R_1}(1 + \dfrac{R_1}{R_2} D)} V_{do} \tag{12}$$

Better sensitivity in the voltage control is obtained from Equation 12 where it should be taken into account that: a) D may vary from zero to one though there is an increase on the harmonic contents with smaller values of D; b) Practical values of R_c are small; for micro-powerplants, this value is around 3.0 Ω; c) R_2 should have a minimum value; ideally, $R_2 \rightarrow 0.0$, but, the peak current levels through the electronic switching device would be unacceptably high; a reasonable practical value is 10.0 Ω.

Plots of Equation 12 is shown in Figure 2 for V_{phase} = 220V, R_1 = 28 Ω , R_2 = 2 Ω and R_c = 2.388 Ω. As it can be observed, the voltage regulation band is very wide between D = 0.26 and D = 0.63 for changes in the AC phase voltage

magnetic saturation on the proportionality between output voltage and rotor speed such that it is enough to monitor changes in the rotor speed by observing only this voltage; III) wide load current changes does not affect the proportionality between rotor speed and load voltage.

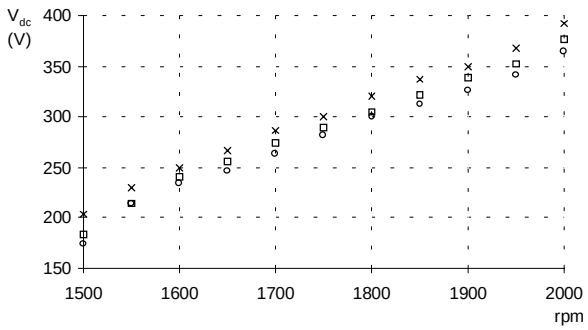

Figure 9 - The terminal voltage (from laboratory tests)

V. Conclusion

A varying load resistance in parallel with the main load of power plants may be an effective way to control rotation and its electrical variables. It offers many desirable characteristics such as robustness, simplicity, modularity, cost reduction, limited short-circuit current, small weight and volume, when compared to the conventional electro-mechanical actuators. Because it is an electronic and compact equipment, this control can be mounted in any position. A microcontroller guarantees optimal immunity against humidity, dust, bad connections and complexity, resulting in a low priced, fast and adaptive response as well energy of good quality.

Other considerations such as quality, technical and economical characteristics and the necessity of simplifying powerplant controls could be also considered. Intermediary results indicate that this control adapts itself very well for the usual load and for the primary energy source conditions producing fast and adequate response. The authors do not see inconveniences for using this type of control with any other type of primary source or load, though tests so far were used only for wind energy.

From the terminal voltage versus load active power characteristics it can be envisaged a safe area inside of which it should be expected moderate rotor speed and reasonable output voltage. The established limits are concerned with rotor maximum overspeed, voltage isolation, primary generated power, tolerable voltage regulation and maximum current through the induction generator windings. There is no need for any shaft encoders or similar for rotor speed measurements since a sensorless algorithm is used to keep the quiescent rotation inside the safe area.

The sensorless speed control proposed in this paper seems to be the best suited for induction generators using electronic control by the load because electrical variables, such as output voltage and load current, have to be acquired all the same for control purposes. This technique is compatible with any type of load, from passive ones to complex autonomous or not autonomous converters. Results obtained so far indicate that with few modifications in the standard control circuitry can produce low regulation of voltage and frequency through control of only the load active power. For powerplants, these two control variables seem to be more appropriate than current control because they use fewer components and, as an advantage, they offer lower voltage regulation for the primary and secondary loads.

VI. References

[1] B. C. Doxey, "Theory and application of the capacitor-excited induction generator", The Engineer magazine, pp. 893-897, Nov/1963.

[2] S. S. Murthy, H. S. Nagaraj e Annie Kuriyan, "Design-based computacional procedures for performance prediction and analysis of self-excited induction generators using motor design packages", IEE Procedings, Vol. 135, Pt B, nº. 1, pp. 8-16, Jan/1988.

[3] G. W. Stagg e A. H. El-Abiad, "Computer methods in power systems analysis", McGraw-Hill Book Company, New York, 1968.

[4] Bonert, R., Hoops, G., “Stand Alone Induction Generator with Terminal Impedance Controller and no Turbine Controls”, IEE Proc. B, 1990.

[5] Farret, F. A., Mello, C. D., “Melhorias na Estrutura e Operação de uma Micro-usina Experimental com Controle Eletrônico pela Carga”, XII National Symposium on Production and Transmission of Electrical Energy, Recife, PE, Proceedings CIGRÉ, Oct./93.

[6] Portolann, C. A., Farret, A. F. and Machado, R. Q., "Electronic Regulation by the Load of the Electrical Variables and Speed of Induction Micro Turbogenerators", IV Congresso Brasileiro de Eletrônica de Potência (COBEP'97), Belo Horizonte, pp 125-129, 1997.

[7] Watanabe, C. H., Barreto, A. N., “Self-Excited Induction Generator Force-Commutated Rectifier System Operating as a DC Power Supply”, IEE Proc., Vol. 134, Pt. B, n° 5, Sep./87.

[8] Bose, B. K., "Power Electronics and Variables Drives". Book, IEEE Press, 1997.